Propagation of the nuclear mean-field uncertainties with increasing distance from the parameter adjustment zone: Applications to superheavy nuclei

I. Dedes[1] and J. Dudek[2,1]

[1]*Institute of Physics, Marie Curie-Skłodowska University, PL-20 031 Lublin, Poland*

[2]*IPHC/DRS and Université de Strasbourg, 23 rue du Læss, B.P. 28, F-67037 Strasbourg Cedex 2, France*

(Received 21 July 2018; revised manuscript received 27 March 2019; published 10 May 2019)

We combine the framework of the inverse problem theory and the Monte Carlo approach to formulate *exact* mathematical models that enable estimates of the uncertainty distributions for modeling predictions. We illustrate and discuss in particular what we refer to as the "NO GO property." When the uncertainties of data constituting the input to the parameter adjustment procedures exceed certain critical value(s), even an *exact* modeling looses its *stochastic reliability*; its further use may provide "acceptably looking" rms deviations in the fitting zone with very likely meaningless, because they are unstable, predictions outside of it. We examine confidence intervals for intraneous (inside of the adjustment zone) and extraneous (outside of the adjustment zone) predictions and we demonstrate that "satisfactory" rms deviations in the intraneous modeling regime offer generally null certitude about the quality of extraneous predictions. Even though not entirely unknown, this property requires strong emphasizing since ignoring it has lead to misleading conclusions and confusing messages in the literature. We generalize our considerations to the realistic nuclear mean-field simulations of the properties of the nucleonic mean-field energies in spherical nuclei. We predict quantitatively the deterioration with increasing mass of the nucleonic-energy confidence intervals in superheavy nuclei. We show a strong dependence of those confidence intervals on the quantum characteristic of nucleonic states and provide detailed illustrations. In particular we demonstrate that, in the realistic predictions for the superheavy nuclei with the phenomenological Woods-Saxon Hamiltonian for up to $Z \approx 114$ or so, one obtains relatively stable predictions of the single-particle spectra with $N \leqslant 180$, while approaching the NO GO zone of this model for further increasing neutron numbers. Thus the main area of today's interest within the instrumental reach for the superheavy nuclei studies remains, according to these estimates for the Woods-Saxon modeling, within the stability zone.

DOI: 10.1103/PhysRevC.99.054310

I. INTRODUCTION

Model prediction capacities and estimates of modeling uncertainties—the subjects of increasing importance in particular in contemporary nuclear physics—are of strong interest in many subfields of physics and technological applications as well as in a quickly developing subfield of applied mathematics: the *inverse problem theory*. Presentation of the general mathematical background of this theory can be found in numerous textbooks (cf. Refs. [1–5]), whereas the most recent progress in the underlying mathematical methods as well as their applications can be followed via specialized journals (see Ref. [6]). The issues of uncertainties, information, and statistics related specifically to nuclear physics have been addressed in Ref. [7].

The issue of reliable parameter estimates for the nuclear structure applications is gaining in importance with a quickly increasing number of published articles on the subject (cf. the recent collection in Ref. [8]). Distinction is being made between analyses of statistical uncertainties performed with various standard mathematical tools (cf. a recent example, Ref. [9]) and the so-called systematic (mainly due to model inaccuracies) ones as discussed in a broader context in Ref. [10]. Certain efforts concentrate on Bayesian-type techniques [11], especially in the case of approaches for which Monte Carlo methods become strongly computer-time-consuming.

The field of application of various methods of estimating the modeling-prediction uncertainties covers the majority of the nuclear structure subfields including the analysis of nuclear masses [12], nuclear skin, [13], effective field theory methods like those in Ref. [14], "traditional" nuclear Skyrme-Hartree-Fock approaches [15–17], and nucleon-nucleon interactions and effective-interaction approaches [18]. Optimization methods addressing the nuclear-energy-density-related algorithms are discussed in, e.g., Refs. [19,20], and uncertainties related to the estimates of the nuclear symmetry energy are discussed in Ref. [21]. One of the important elements in optimization approaches is related to reduction of the parameter spaces in the case of overparametrized models, the issue pertinent to many effective nuclear physics Hamiltonians (cf. Refs. [22–24]) in the context of the energy density functionals (cf. also Refs. [25,26]).

Here we limited ourselves to citing just a few examples illustrating a dynamic evolution of this field of research.

In the present article we address a specific nuclear physics subject in the domain of predictive inference within the mean-field theory: predicting the future observations based on the past observations as well as on the information about the errors or uncertainties of the latter. More precisely, we are interested in predictions for exotic nuclei lying on the (Z, N) plane further and further away from the nuclei that have been used to adjust the Hamiltonian parameters.

Intuitively, one usually expects that prediction uncertainties increase for more and more exotic nuclei. In the present article we focus on quantifying these expectations by providing model-dependent, but realistic, numbers while employing the realistic experimental sampling and an as stable as possible theoretical modeling algorithm. Because the main interest of the article is *not* the construction of the new interactions but rather studying the inference process, the particular form of the Hamiltonian plays a secondary role, provided it can be considered empirically realistic.

In contemporary nuclear structure calculations, in particular, for exotic nuclei, extensive use is made of modeling of the total nuclear energies, potential barriers, quasiparticle excitations, rotational-band properties, etc. These quantities are frequently used in comparisons of the mean-field theory predictions with experiment. The underlying element contributing to good quality for this type of the mean-field theory calculations is reliable mean-field single-particle energies. In this article we select as observables of interest for the modeling the single-particle nucleon energies in spherical nuclei. We focus on the estimates of the *confidence intervals* of the single-particle energies, in particular, by examining the propagation of the experimental single-particle energy uncertainties with increasing mass number or isospin of nuclei at the frontiers of today's research in this domain.

According to the inverse problem theory, prediction capacities of the modeling depend in an essential manner on two elements: the mathematical model itself and the selection (sampling) of the experimental data. For a defined model it is the sampling and the quality of the data that determine the quality of the "resulting optimal parameters of the model." Our model of choice is the spherical Woods-Saxon Hamiltonian. It has been used for many decades in nuclear physics and has shown certain advantages in the phenomenological description of single-nucleon energies. Examples of applications in a context similar to ours can be found in Ref. [27], where the method of preparing the experimental data for comparison with the modeling results has been presented (cf. Sec. 2 of Ref. [27]).

To be able to address these issues on a more detailed level, in what follows we introduce, after Ref. [27], the notion of the so-called *intraneous* and *extraneous* predictions. Here we avoid using terms such as "interpolation" or "extrapolation," which have a reserved meaning in mathematics and their use would be incorrect in the present context. In the case of nuclear physics applications, we refer to "intraneous predictions" when performing the calculations for unknown nuclei or observables inside of the known areas (as if interpolating) and extraneous otherwise (as if extrapolating). The latter may refer to exotic, e.g., superheavy nuclei, usually (far) away from the known nuclear areas on the (Z, N) plane, or to the deeper and deeper bound nucleonic levels, further and further away from the known ones used for the fitting of the Hamiltonian parameters.

II. CONSIDERATIONS BASED ON AN EXACT TOY-MODEL

It is instructive to present first the results of an exact toy-model, which shows certain distinct features of intraneous and extraneous predictions just introduced. In particular, this "academic looking" model reveals very important robust mathematical characteristics of the predicting mechanism, which may at first glance look paradoxical: Any *even exact modeling*, no matter the physics application, may lose any prediction capacities for certain data sampling or sufficiently far from the adjustment zone. We refer to this situation as the NO GO property or the NO GO asymptotic.

Consider a set of numbers which play the role of experimental data, $f_i^{\rm exp} = f_i \pm \delta f_i$ for $i = 1, 2, \ldots, n_s$. By construction of the present model we set $f_i \equiv \exp(x_i)$, where x_i are some known real numbers defined for the sake of this discussion (see below), whereas δf_i represent error bars. The related errors are assumed to be normal distributed, $\delta f_i \approx \mathcal{N}(\mu_i, \sigma_i)$, centered at $\mu_i \equiv f_i$. We assume δf_i as known, and alternatively, we assume μ_i and σ_i as given.

As the next step let us introduce a *modeling function* of the set $\{f_i^{\rm exp}\}$ defined by (cf. Ref. [28])

$$F(x_i; p) \equiv A + Bx_i + C\sinh(x_i) + D\cosh(x_i). \tag{1}$$

It depends on four parameters, $\{A, B, C, D\} \equiv p$, and defines an exact model because for vanishing errors we have

$$f_i = F(x_i, p|_{A=0,B=0,C=1,D=1}) \text{ for any } x_i. \tag{2}$$

In the illustration which follows we set $n_s = 5$ sampling points defined with the help of reference values: $x_i^r = 0$, 0.1, 0.2, 0.3, and 0.4, for $i = 1$, 2, 3, 4, 5, respectively. The resulting "experimental reference input data" are $f_i^r \equiv \exp(x_i^r) \approx 1$, 1.11, 1.22, 1.35, and 1.49. They play the role of five exact reference-solutions of the model. Of course the above choice is arbitrary and the role of the specific values is merely to allow for some explicit numerical applications.

In the spirit of the Monte Carlo approach we generate the distributions $\delta\varphi_i \approx \mathcal{N}(\mu_i, \sigma_i)$ composed of $N_{\rm MC} \approx 10^5$ random, normally distributed numbers representing the uncertainties δf_i, for $i = 1, 2, \ldots, n_s$. In other words, we generate $\{\delta\varphi_i; i = 1, 2, \ldots, n_s\}_k$ n_s-plets for $k = 1, \ldots, N_{\rm MC} \approx 10^5$ and minimize $N_{\rm MC}$ times the corresponding χ^2 test with $[f_i^{\rm exp} = f_i + \delta\varphi_i]$:

$$\chi^2(A, B, C, D) \propto \sum_{i=1}^{n_s} \left[f_i^{\rm exp} - F(x_i; A, B, C, D)\right]^2. \tag{3}$$

In what follows we use $\sigma_i = \sigma$, i.e., independent of i, and the proportionality can be replaced by equality without influencing the minimization results (here and in the following we use the Levenberg-Marquard minimization algorithm, the choice that in no respect influences the calculation results).

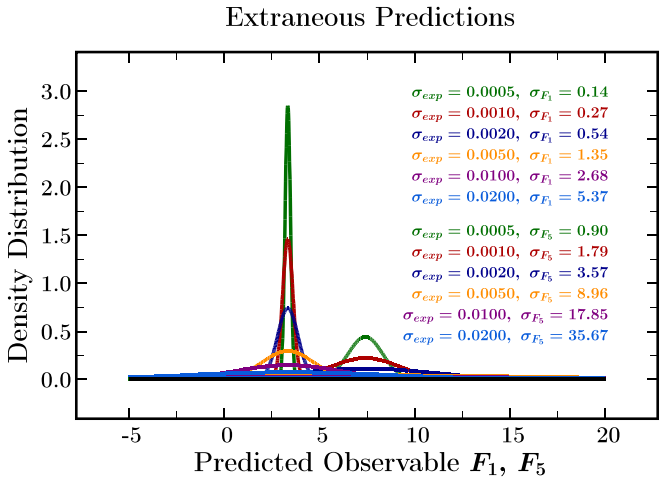

FIG. 1. Illustration of the uncertainty probability distributions of the extreme extraneous test values, the smallest, F_1, and the largest, F_5, discussed in the text; cf. Table I for a more complete presentation.

We obtain $N_{\rm MC}$ quadruplets of model parameters $\{A, B, C, D\}_k$. With the latter ones known, we construct the *occurrence probability* histograms allowing us to determine the most probable value of each parameter, the corresponding confidence intervals, etc. The so-prepared mathematical model is used for testing the extraneous and intraneous predictions.

We begin with the *extraneous prediction properties* and introduce the auxiliary arguments $X_j^e = 1.2,\ 1.4,\ 1.6,\ 1.8,$ and 2.0 outside of the intraneous interval $\{x_i\} \in [0, 0.4]$, and the corresponding $F_j \equiv \exp(X_j^e) \approx 3.32, 4.06, 4.95, 6.06,$ and 7.39, the latter serving as the exact solutions for the extraneous data. The calculated Monte Carlo distributions for the smallest and the largest test values, F_1 and F_5, respectively, are shown in Fig. 1, whereas the full set of the extraneous data points and the confidence intervals is given in Table I. In this illustration the standard-deviation uncertainties σ_{F_i} are calculated by employing the Monte Carlo approach with $\sigma_i = \sigma = 0.0005,$ 0.001, 0.002, 0.005, 0.01, and 0.02, for $i = 1, 2, \ldots, 5$.

Let us emphasize that even though the discussed model is by construction *exact*, and thus capable of reproducing the mathematical truth exactly under the assumption of the vanishing errors—the latter situation will *never* be achieved outside of the purely mathematical considerations because there errorless experimental data do not exist. As a matter of fact the latter observation applies generally and in this respect *de facto* removes differences between the so-called exact and inexact modeling.

Still within the exact-modeling context, increasingly poor quality of the data will generally lead to exceeding any *maximum prediction uncertainty* treated by the user of the model as acceptable within her or his given context. In constructing the modeling predictions, usually the uncertainty interval of each of the predicted observables F_κ should not exceed the physicist-defined limit L_κ. When at least one limit is exceeded, the model can be considered not applicable anymore to predicting observables in the physicist-defined context. In the case of the exact modeling we arbitrarily refer to this mechanism as the NO GO limit. Whereas a similar mechanism applies for the in-exact modeling, very likely even more restrictively, in the case of the *exact model* the impossibility of applying such a model for predicting may appear paradoxical.

Table II shows the A, B, C, and D model parameters with the corresponding standard deviations obtained using the Monte Carlo approach. One can notice that the confidence intervals of the parameters broaden quickly with increasing σ, a measure of the "experimental data error" within the model. This behavior should be confronted with the *excellent performance of the model* in terms of confidence intervals in the intraneous range visible from Table III.

Table III shows the results strictly analogous to those in Table I but for the reference (intraneous) zone with f_i lying in between the reference points f_i^r to which the parameters are adjusted. Despite very wide confidence intervals in the case of F_i, the predictions for f_i are precise within four decimals whereas the standard deviations are 3 to 4 orders of magnitude better. Let us emphasize that the A, B, C, and D parameter uncertainty distributions are common for the f's and the F's. This information should be confronted with "disastrously poor" confidence in the case of parameters in Table II, at least for some σ values. One must conclude that the same quality of parameter incertitude, even "disastrously" large, may still provide excellent or very poor predictions depending on whether one is considering the intraneous or the extraneous prediction zone.

An implication is that one must not conclude about the quality of the extraneous variant of the simulation from the quality of the intraneous one. All these predictions must be studied separately on a case-by-case basis. Let us emphasize that precisely this particular property leads to serious

TABLE I. We use the simplifying assumption $\sigma_i \to \sigma$, first column, for various σ, the latter mimicking experimental errors. It is up to the physicist to decide which value of the prediction confidence interval σ_{F_i} is still acceptable in the context. When the modeling errors exceed that value, the *exact* model in question becomes *unacceptable anymore*—the situation we refer to as the NO GO limit for "exact modeling."

σ	$F_1 \pm \sigma_{F_1}$	$F_2 \pm \sigma_{F_2}$	$F_3 \pm \sigma_{F_3}$	$F_4 \pm \sigma_{F_4}$	$F_5 \pm \sigma_{F_5}$
0.0005	3.32 ± 0.13	4.06 ± 0.24	4.95 ± 0.39	6.06 ± 0.61	7.39 ± 0.90
0.0010	3.32 ± 0.27	4.06 ± 0.48	4.95 ± 0.78	6.06 ± 1.21	7.39 ± 1.79
0.0020	3.32 ± 0.53	4.06 ± 0.95	4.95 ± 1.56	6.06 ± 2.41	7.39 ± 3.56
0.0050	3.32 ± 1.34	4.06 ± 2.39	4.95 ± 3.91	6.06 ± 6.04	7.39 ± 8.92
0.0100	3.32 ± 2.68	4.06 ± 4.81	4.95 ± 7.87	6.06 ± 12.2	7.39 ± 17.9
0.0200	3.32 ± 5.39	4.06 ± 9.60	4.95 ± 15.7	6.06 ± 24.3	7.39 ± 35.8

TABLE II. The uncertainty ranges of the exact $\{A = 0, B = 0, C = 1, D = 1\}$ parameter values with their standard-deviation uncertainties obtained using various values of σ. Observe that the exact model in Eq. (2) has been chosen as a sum of even $[A + D\cosh(x)]$ and odd $[Bx + C\sinh(x)]$ terms modeling $\exp(x)$, which is neither even nor odd. It turns out that in the considered case the standard deviations of A are approximately equal to those of D (similarly those of B and those of C).

σ	$A \pm \sigma_A$	$B \pm \sigma_B$	$C \pm \sigma_C$	$D \pm \sigma_C$
0.0005	0.00 ± 0.16	0.00 ± 0.79	1.00 ± 0.81	1.00 ± 0.16
0.0010	0.00 ± 0.32	0.00 ± 1.59	1.00 ± 1.61	1.00 ± 0.32
0.0020	0.00 ± 0.64	0.00 ± 3.16	1.00 ± 3.21	1.00 ± 0.64
0.0050	0.00 ± 1.60	0.00 ± 7.91	1.00 ± 8.02	1.00 ± 1.60
0.0100	0.00 ± 3.24	0.00 ± 15.9	1.00 ± 16.2	1.00 ± 3.24
0.0200	0.00 ± 6.45	0.00 ± 31.8	1.00 ± 32.2	1.00 ± 6.45

misunderstandings and lies at the origin of inconsistent predictions or conclusions in the literature.

It is worth emphasizing at this point a danger of mistaking an "acceptable" quality[1] of the rms deviations resulting from the χ^2 fit with the affirmation of a "good" quality of predictive power (note the quotation marks emphasizing the presence of an arbitrary judgment). The reader may consult a much more recent discussion, Ref. [30], showing a number of instructive examples. In the rest of this article we examine a number of features that reveal a certain statistical significance that can be attached to the results of modeling predictions.

However before proceeding further let us emphasize that the particular choice of the exponential as the generating function to construct the exact model discussed so far has no impact whatsoever on the discussed general features of the exact modeling. First, in many cases of nonexponential models the divergencies of the predictions are themselves exponential in character, thus relatively fast. Second, by choosing the repartition of the characteristic points of the model in the intraneous and/or extraneous zones, one can make the local features of functioning of the particular model resemble those with other (nonexponential) generating functions.

III. CONSIDERATIONS BASED ON THE REALISTIC PHENOMENOLOGICAL MEAN-FIELD HAMILTONIAN

In what follows we examine the stochastic features of the modeling prediction capacities in the context of *a realistic nuclear mean-field approach* using the Monte Carlo method. For this purpose we chose the standard, nuclear mean-field Woods-Saxon Hamiltonian:

$$\hat{H} = \hat{T} + \hat{V}_{\rm WS} + \hat{V}^{\rm so}_{\rm WS} + [\hat{V}_{\rm Coulomb} \text{ for protons}]. \quad (4)$$

[1]The problem of very likely statistical insignificance of the "good looking" χ^2 fit is a rather long-standing issue, cf. Ref. [29], whose authors observe with sarcasm: "Unfortunately, many practitioners of the parameter estimation never proceed beyond determining the numerical values of the parameter fit. They deem a fit acceptable if a graph of data and model 'look good'. This approach is known as chi-by-the-eye. Luckily, its practitioners get what they deserve."

TABLE III. Results analogous to those in Table I but for intraneous predictions; f_i values are exact values For details, see text.

σ	$f_1 \pm \sigma_{f_1}$	$f_2 \pm \sigma_{f_2}$	$f_3 \pm \sigma_{f_3}$
0.0005	1.1618 ± 0.0004	1.2840 ± 0.0004	1.4191 ± 0.0004
0.0010	1.1618 ± 0.0008	1.2840 ± 0.0008	1.4191 ± 0.0008
0.0020	1.1618 ± 0.0016	1.2840 ± 0.0016	1.4191 ± 0.0016
0.0050	1.1618 ± 0.0039	1.2840 ± 0.0040	1.4191 ± 0.0040
0.0100	1.1618 ± 0.0078	1.2840 ± 0.0079	1.4191 ± 0.0080
0.0200	1.1618 ± 0.0158	1.2840 ± 0.0158	1.4191 ± 0.0160

Above, $\hat{T}$ represents the kinetic energy operator and $\hat{V}_{\rm WS}$ represents the central Woods-Saxon potential

$$\hat{V}_{\rm WS} = \frac{V^c}{1 + \exp[(r - R^c)/a^c]}, \quad (5)$$

where V^c denotes the central potential depth parameter and r^c in $R^c = r^c A^{1/3}$ is the central radius parameter. Similarly a^c is referred to as the central diffusivity parameter. The spin-orbit potential has the usual form

$$\hat{V}^{\rm so}_{\rm WS} = \frac{1}{r}\frac{dV_{\rm so}(r)}{dr}\,\hat{\ell}\cdot\hat{s}, \quad (6)$$

where

$$V_{\rm so}(r) = \frac{\lambda^{\rm so}}{1 + \exp[(r - R^{\rm so})/a^{\rm so}]}, \quad (7)$$

and where $\lambda^{\rm so}$ is the spin-orbit strength-, $r^{\rm so}$ in $R^{\rm so} = r^{\rm so}A^{1/3}$ is the spin-orbit radius-, and $a^{\rm so}$ is the spin-orbit diffusivity parameter. It follows that the model depends on two sets of six parameters,

$$\{V^c, r^c, a^c, \lambda^{\rm so}, r^{\rm so}, a^{\rm so}\}_{\pi,\nu}, \quad (8)$$

one for the protons, π, and one for the neutrons, ν.

The Hamiltonian in Eq. (4) has been selected here because of its simplicity, its realistic empirical performance vs experiment, and its negligible CPU time-computing requirements. It is used to construct *an exact and realistic model* for stochastic Monte Carlo simulations. For this purpose we first adjust the two parameter sets in Eq. (8) by performing a χ^2 fit to the experimentally known single-particle levels in ^{208}Pb:

$$\text{Neutrons}: \{2f_{7/2}, 1i_{13/2}, 3p_{3/2}, 2f_{5/2}, 3p_{1/2}, 2g_{9/2}, 1i_{11/2}, 3d_{5/2}, 2g_{7/2}, 4s_{1/2}, 3d_{3/2}\}_\nu, \quad (9)$$

and

$$\text{Protons}: \{1h_{11/2}, 2d_{3/2}, 3s_{1/2}, 1h_{9/2}, 2f_{7/2}, 1i_{13/2}, 2f_{5/2}\}_\pi. \quad (10)$$

In this way we construct the *reference parameter sets* $\{p^{\rm ref}\}_{\pi,\nu}$. From now on the corresponding calculated energy levels $\{e^{\rm ref}\}_{\pi,\nu}$ can be treated as the exact solutions of the reference modeling. Because in the following part of the discussion their role is to replace the real experimental data in the parameter adjustments, they are referred to as *pseudoexperimental data*.

To construct the Monte Carlo modeling of experimental uncertainties we introduce Gaussian uncertainty distributions

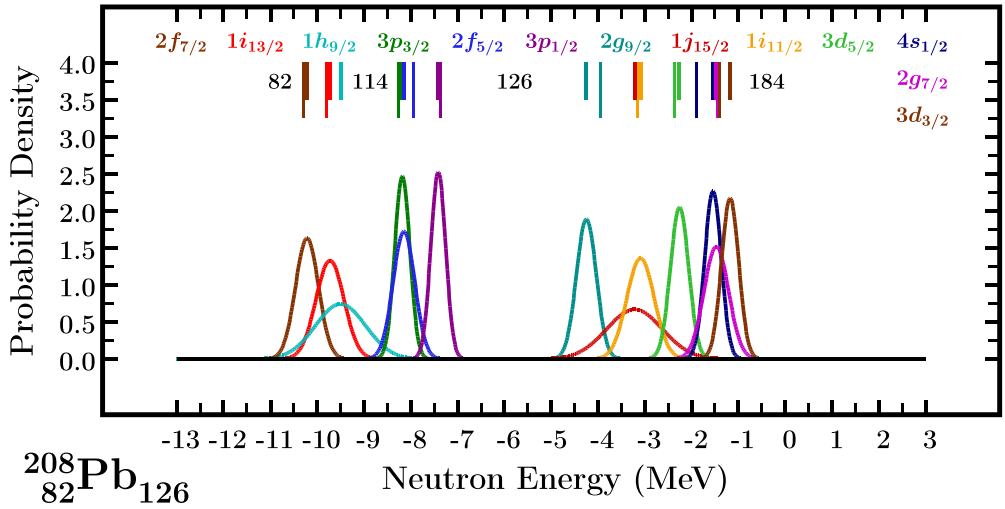

FIG. 2. Normalized, smoothed histograms showing the MonteCarlo-simulated probability distributions of uncertainties for the neutron single-particle energies within $N_{\rm sh} = 5$ and $N_{\rm sh} = 6$ main shells of the ^{208}Pb nucleus. The average experimental-level uncertainty assumed here was $\sigma^{\rm ref} = 0.3$ MeV. The 11 experimental neutron levels are those listed in Eq. (9) with the numerical energy values extracted from "raw" experimental data as in Ref. [27], where the original information comes from Refs. [31–36]. The long bars give the experimental energies. Missing long bars for $1h_{9/2}$ and $1j_{15/2}$ levels signify missing experimental information. For comparison, the short bars show the positions of the peaks of the distributions.

of the exact pseudoexperimental levels, thus simulating experimental errors within an exact model. For this purpose we generate numerically the Gaussian distributions, here of a common width $\sigma^{\rm ref}$, which corresponds to σ in the exact modeling discussed earlier. Following Ref. [27] the average experimental uncertainty for the eight spherical nuclei considered here, i.e., ^{16}O, ^{40}Ca, ^{48}Ca, ^{56}Ni, ^{90}Zr, ^{132}Sn, ^{146}Gd and ^{208}Pb, can be estimated with the result close to 300 keV. Therefore we set $\sigma^{\rm ref.} = 300$ keV as a "reasonable" order of magnitude estimate for uncertainties of experimental (input) data. In this way we construct what is usually referred to as "noisy" data. In the spirit of the Monte Carlo approach we generate Gaussian-distributed random sets of the new pseudoexperimental data $N_{\rm MC} \approx 10^5$ times. Repeating the χ^2 fit, each time we obtain a new set of parameters, $p^{\rm MC}$, and a new set of single-particle energies, $\{e^{\rm MC}\}$, with the help of which we construct the occurrence probability histograms illustrated in Fig. 2 for the neutrons and in Fig. 3 for the protons.

Figure 2 shows the uncertainty distributions of the neutron single-particle energies of ^{208}Pb$_{126}$. Levels $1h_{9/2}$ and $1j_{15/2}$, not known experimentally, were not taken into account in determining the reference parameters—but remarkably, their uncertainty distributions happen to be approximately twice as broad as the average of the others (we return to this issue at the end of the article). Observe that the next broadest distributions correspond to big-ℓ orbitals, $1i_{13/2}$ and $1i_{11/2}$, with $\ell = 6$.

Turning to the predictions related to single-nucleon spectroscopic properties in the superheavy nuclei, which in the present context are qualified as extraneous prediction, our

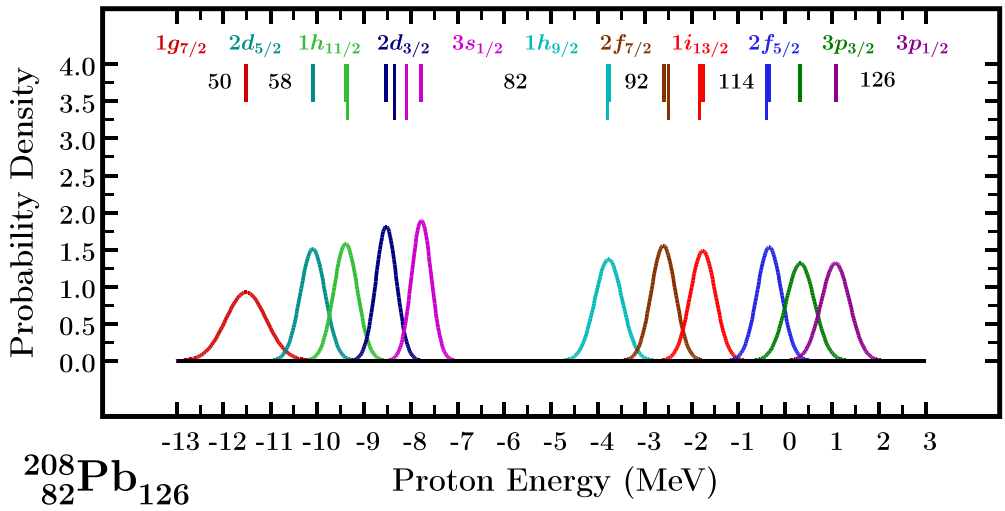

FIG. 3. Similar to the preceding one but for the proton $N_{\rm sh} = 4$ and $N_{\rm sh} = 5$ main shells of the ^{208}Pb nucleus.

TABLE IV. Realistic Monte Carlo calculation results of the FWHM values (in MeV) of the neutron single-particle levels covering the nuclear main shells $N_{\rm sh} = 5$ and 6 for the Fl_{114} superheavy isotopes indicated. The ^{208}Pb results have been extracted from the curves in Fig. 2, where the average experimental uncertainty was approximated by $\sigma_{\rm ref} = 0.300$ MeV. Recall that in about 90 flerovium atoms observed so far, the neutron numbers correspond to $N \in [170, 176]$. The present table with the range of N as given is meant, in the first place, to illustrate the modeling method and the associated extraneous prediction instability properties. The formulation presented at this point satisfies the mathematical criteria of the exact modeling; for details, see text.

Z	N	$2f_{7/2}$	$1i_{13/2}$	$1h_{9/2}$	$3p_{3/2}$	$2f_{5/2}$	$3p_{1/2}$	$2g_{9/2}$	$1j_{15/2}$	$1i_{11/2}$	$3d_{5/2}$	$4s_{1/2}$	$2g_{7/2}$	$3d_{3/2}$
82	126	0.58	0.71	1.27	0.38	0.55	0.37	0.50	1.40	0.69	0.46	0.41	0.62	0.43
114	164	0.75	0.88	1.68	0.53	0.68	0.51	0.52	0.92	1.03	0.39	0.38	0.53	0.43
114	170	0.83	0.89	1.70	0.61	0.77	0.60	0.48	0.80	1.00	0.32	0.30	0.47	0.35
114	172	0.86	0.91	1.71	0.65	0.81	0.64	0.48	0.76	1.00	0.32	0.30	0.48	0.35
114	180	1.03	1.03	1.78	0.84	0.99	0.83	0.58	0.71	1.05	0.42	0.39	0.57	0.42
114	184	1.12	1.10	1.82	0.94	1.10	0.93	0.66	0.73	1.10	0.50	0.46	0.64	0.50
114	196	1.41	1.37	2.00	1.25	1.41	1.24	0.93	0.89	1.29	0.78	0.73	0.92	0.76
114	214	1.86	1.79	2.32	1.70	1.87	1.69	1.37	1.27	1.67	1.20	1.13	1.35	1.16
114	228	2.19	2.12	2.59	2.03	2.20	2.02	1.68	1.59	1.97	1.50	1.41	1.66	1.45

simulations show the detailed estimates of the confidence intervals with increasing neutron number of the isotope. In particular, Table IV shows the full width at half maximum (FWHM) of the uncertainty distributions for the predicted neutron levels in the main neutron shells between $N = 126$ and $N = 228$. Analogous results for the protons are displayed in Table V.

Let us notice that, generally, the FWHM values of the uncertainty distributions do *not* change *in any monotonic or otherwise regular manner*, neither as functions of the orbital angular momentum ℓ nor as functions of the neutron number N. Following the results of tests performed here (which can be considered as realistic estimates) the average tendencies can be characterized as follows. First, one may note an increase in the confidence intervals by factors varying between 2 and 4, when the neutron number varies between $N = 126$ and $N = 228$. Second, the uncertainties of the predictions, after the first zone of relative stability for $N \in [164, 184]$, increase faster when the neutron number increases. In particular for the deeply bound levels the confidence intervals (not shown) increase quickly up to about 4.5 MeV for the lowest, $1s_{1/2}$, level.

At the same time, the variation of (certain) single-particle energies with varying parameters of the Hamiltonian is getting much stronger at growing N, manifesting a kind of "relative oversensitivity" as compared to the light isotopes with the narrower confidence intervals. This can be seen as an expression of the fact that the distant [in terms of the (Z, N) plane] data constrain the model relatively weaker.

To obtain a quantitative illustration of the above statement we illustrate in Fig. 4 variations of the predicted single-particle energies in Fl isotopes following the uncertainty variation of the pseudoexperimental level $1h_{9/2}$. This particular level represents also a particular interest because its experimental position remains so far unknown but hopefully will be measured in the near future. Therefore it is instructive to follow the expected modification of the predictions depending on the actual value of the yet unknown datum. Results show that whereas the majority of the predicted energy positions in the lighter $Z = 114$ isotope considered, relatively close to the fit zone, vary only little with the ^{208}Pb-fit uncertainties, the energies of the same levels in the heavy isotope vary significantly stronger. This shows that the induced prediction uncertainties also for the single-particle energies (in addition to the widths of the uncertainty probability distributions) increase with the increasing distance from the fitting zone.

More precisely, concerning the "practical aspects" related to the prediction uncertainties for the superheavy nuclei obtained using the Woods-Saxon phenomenological modeling

TABLE V. Realistic Monte Carlo calculation results of the FWHM values (in MeV) of the proton single-particle levels covering the nuclear main shells $N_{\rm sh} = 4$ and 5 for the Fl_{114} superheavy isotopes indicated—to be compared with Table IV.

Z	N	$1g_{7/2}$	$2d_{5/2}$	$1h_{11/2}$	$2d_{3/2}$	$3s_{1/2}$	$1h_{9/2}$	$2f_{7/2}$	$1i_{13/2}$	$2f_{5/2}$	$3p_{3/2}$	$3p_{1/2}$
82	126	1.01	0.62	0.59	0.52	0.50	0.69	0.60	0.63	0.61	0.71	0.71
114	164	0.94	0.56	0.61	0.49	0.47	0.69	0.60	0.60	0.63	0.71	0.71
114	170	1.03	0.64	0.66	0.55	0.52	0.67	0.53	0.51	0.51	0.60	0.59
114	172	1.07	0.68	0.69	0.58	0.55	0.68	0.53	0.50	0.49	0.62	0.56
114	180	1.24	0.87	0.85	0.77	0.73	0.79	0.59	0.53	0.49	0.55	0.50
114	184	1.35	0.98	0.95	0.88	0.83	0.88	0.66	0.59	0.54	0.58	0.53
114	196	1.67	1.31	1.25	1.21	1.16	1.18	0.93	0.85	0.80	0.79	0.73
114	214	2.16	1.80	1.72	1.72	1.66	1.67	1.38	1.31	1.27	1.22	1.17
114	228	2.52	2.16	2.07	2.09	2.02	2.05	1.73	1.66	1.63	1.56	1.51

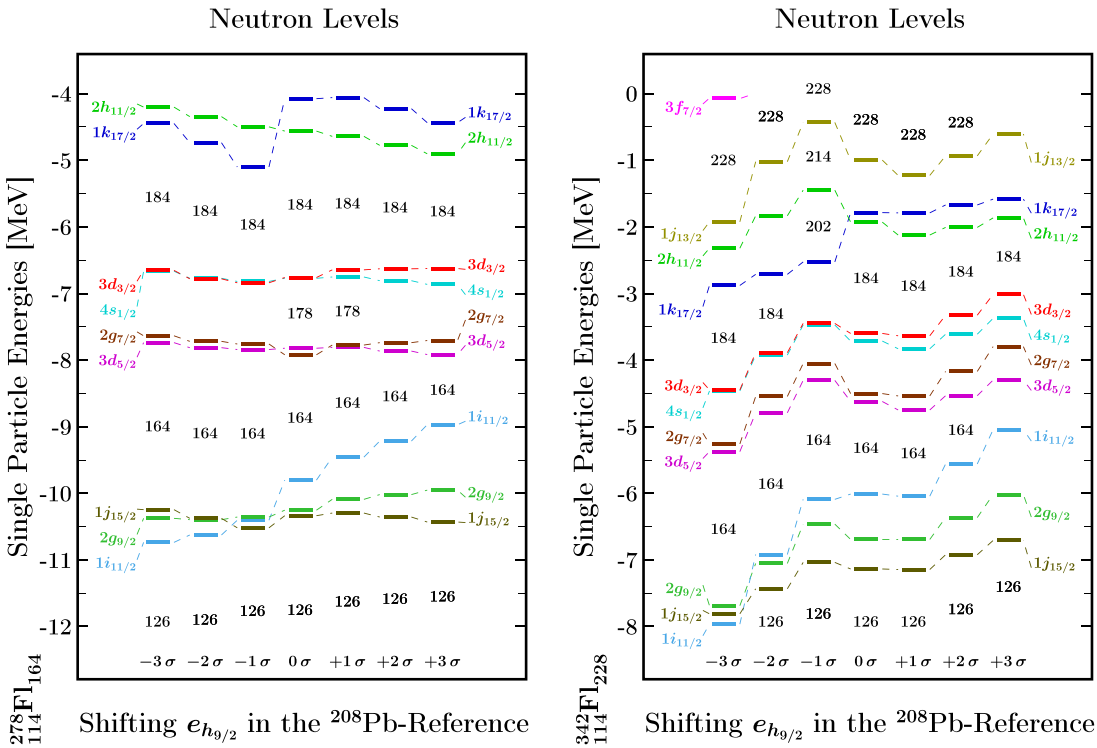

FIG. 4. Illustration of the prediction instability for the energy values of the single-particle levels as a reaction to a single input-level uncertainty. The energy of the pseudoexperimental neutron level $h_{9/2}$ (experimental result not known) has been shifted with respect to the starting position by multiples of the standard deviation ($\pm\sigma$, $\pm 2\sigma$, and $\pm 3\sigma$, where $\sigma \leftrightarrow \sigma_{\text{ref}} = 0.3$ MeV). Each time the parameters of the Hamiltonian were readjusted for the ^{208}Pb data. As it can be seen from the left-hand panel, the majority of the levels in the ^{278}Fl behave in a rather stable and regular manner, varying little, except for the $1i_{11/2}$ and $1k_{17/2}$ states. Behavior of the single-particle energies in the ^{342}Fl nucleus, right-hand panel, shows much more sensitivity, indicating that the predictions of the energy positions in a nucleus placed further away from the parameter adjustment zone must be considered significantly more unstable.

we may conclude that, in the vicinity of $Z \approx 114$, the predictions can be considered relatively stable up to $N \approx 184$, whereas for still increasing N values we approach the model's NO GO zone with the impossibility of stable predictions. This conclusion may be considered optimistic or reassuring because this predicted stability area covers most of the nuclei of interest from the current experiment's view point.

IV. SUMMARY AND CONCLUSIONS

We have studied the application of the Monte Carlo technique to produce realistic estimates of the confidence intervals of the nucleonic mean-field energies and, more generally, the uncertainty probability distributions. With the help of the exactly soluble mathematical model we have illustrated the fundamental importance in distinguishing between what we refer to as *intraneous* and *extraneous* modus operandi when constructing model predictions. In the nuclear structure applications, the intraneous predictions refer to addressing either the predictions of single-nucleon levels in between those known already from experiment or the predictions for nuclei lying, on the (Z, N) plane, in between the ones known experimentally. The extraneous predictions in turn correspond either to nuclei away from the known area—the case of exotic and superheavy nuclei—or to the single-nucleon levels well below or well above the ones known experimentally and used for the parameter adjustment. Illustrative examples show that from the fit quality in the intraneous regime (usually "excellent") strictly nothing can be said with certainty about the predictions for the extraneous modus operandi, for which case dedicated tests must be programmed.

In contemporary quantum physics and in nuclear structure physics in particular, the so-called *exact theory or modeling* attract a certain special aura and interest. Because all theories depending on parameters rely on the use of the inverse problem techniques, and because there exist no errorless experimental data to which parameters are fitted, it becomes clear that all theories with adjustable parameters become unconditionally inexact. This is simply because the "exact parameter values of exact theories" remain unknown—and this independently of the conceptual advancement and/or complexity of the theory. Using mathematical-modeling techniques we have examined and emphasized the presence of a practical limitation referred to as the NO GO property: There always exists a critical value of the experimental uncertainty, beyond which even a hypothetically exact theory becomes impractical in any physicist-predefined context. This happens when the poor quality data do not constrain the theory sufficiently to bring the parameters with the necessary precision to the "physical range of interest."

To estimate the confidence intervals of the mean-field single-nucleon energies in the chain of superheavy nuclei we have used the Monte Carlo techniques and the empirically successful, realistic Woods-Saxon nuclear mean-field model, particularly well suited for this kind of modeling due to its negligible computer CPU-time requirements and parametric stability properties. For this purpose we have used the concept of pseudoexperimental levels and the exact-modeling principles. Illustrations for a long chain of flerovium ($_{114}$Fl) isotopes indicate that uncertainties grow very quickly with increasing neutron number, whereas for $N = 164$ the confidence intervals of the individual levels remain, on the average, close to those of the reference nucleus ^{208}Pb; their values increase up to a factor of 4 at the shell closure $N = 228$. This implies that the uncertainty distributions are getting considerably broader and strongly overlapping and consequently the stochastic reliability of the predictions should be considered much poorer as compared to the lighter superheavy nuclei illustrated in this article. It could be improved only via introduction of the new experimental data and in particular by narrowing the experimental uncertainties (error bars).

The present article can be seen as a pilot project limited to the detailed analysis of the uncertainty aspects; the implication for the large-scale nuclear structure calculations in exotic nuclei using these concepts are in progress and will be reported elsewhere.

ACKNOWLEDGMENTS

One of the authors, J.D., performed part of this work within the EMPIR Project No. 15SIB10 MetroBeta. This project has received funding from the EMPIR program co-financed by the Participating States and from the European Union Horizon 2020 research and innovation program. This work was partially supported by the Polish National Science Centre (PL) under Contract No. 2016/21/B/ST2/01227.

[1] R. C. Aster, B. Borchers, and C. H. Thurber, *Parameter Estimations and Inverse Problems* (Elsevier Academic, San Diego, 2005).
[2] C. R. Vogel, *Computational Methods for Inverse Problems* (SIAM, Philadelphia, 2002).
[3] A. Tarantola, *Inverse Problem Theory and Methods for Model Parameter Estimation* (SIAM, Philadelphia, 2005).
[4] A. Kirsch, *An Introduction to the Mathematical Theory of Inverse Problems*, Applied Mathematical Sciences (Springer, New York, 2005).
[5] A. A. Samarskii and P. N. Vabishchevich, *Numerical Methods for Solving Inverse Problems of Mathematical Physics* (de Gruyter, Berlin, 2007), Vol. 52.
[6] The progress in the field of the "inverse problem" mathematical methods as well as applications can be followed via specialized journals, e.g., *Inverse Problems* (IOPP), *Journal of Inverse and Ill-posed Problems* (De Gruyter), and *Inverse Problems in Science and Engineering* (Taylor & Francis). For the general mathematical background underlying the aspects of the inverse problem addressed in this article, cf., e.g., Refs. [1–5].
[7] J. Piekarewicz, W.-C. Chen, and F. J. Fattoyev, J. Phys. G: Nucl. Part. Phys. **42**, 034018 (2015).
[8] D.-G. Ireland and W. Nazarewicz, J. Phys. G: Nucl. Part. Phys. **42**, 030301 (2015).
[9] B. D. Carlsson, Phys. Rev. C **95**, 034002 (2017).
[10] J. Dobaczewski, W. Nazarewicz, and P.-G. Reinhard, J. Phys. G: Nucl. Part. Phys. **41**, 074001 (2014).
[11] D. Higdon, D. J. McDonnell, N. Schunck, J. Sarich, and S. M. Wild, J. Phys. G: Nucl. Part. Phys. **42**, 034009 (2015).
[12] J. Toivanen, J. Dobaczewski, M. Kortelainen, and K. Mizuyama, Phys. Rev. C **78**, 034306 (2008).
[13] P.-G. Reinhard and W. Nazarewicz, Phys. Rev. C **81**, 051303(R) (2010).
[14] R. J. Furnstahl, D. R. Phillips, and S. Wesołowski, J. Phys. G: Nucl. Part. Phys. **42**, 034028 (2015).
[15] J. Erler and P.-G. Reinhard, J. Phys. G: Nucl. Part. Phys. **42**, 034026 (2015).
[16] P. Klüpfel, P.-G. Reinhard, T. J. Bürvenich, and J. A. Maruhn, Phys. Rev. C **79**, 034310 (2009).
[17] P.-G. Reinhard, Phys. Scr. **91**, 023002 (2016).
[18] R. Navarro Pérez, J. E. Amaro, and E. Ruiz Arriola, J. Phys. G: Nucl. Part. Phys. **42**, 034013 (2015).
[19] M. Kortelainen, T. Lesinski, J. Moré, W. Nazarewicz, J. Sarich, N. Schunck, M. V. Stoitsov, and S. Wild, Phys. Rev. C **82**, 024313 (2010).
[20] N. Schunck, J. D. McDonnell, D. Higdon, J. Sarich, and S. M. Wild, Eur. Phys. J. A **51**, 169 (2015).
[21] C. J. Horowitz, E. F. Brown, Y. Kim, W. G. Lynch, R. Michaels, A. Ono, J. Piekarewicz, M. B. Tsang, and H. H. Wolter, J. Phys. G: Nucl. Part. Phys. **41**, 093001 (2014).
[22] M.-K. Transtrum and P. Qiu, Phys. Rev. Lett. **113**, 098701 (2014).
[23] T. Niksić and D. Vretenar, Phys. Rev. C **94**, 024333 (2016).
[24] T. Niksić, M. Imbrisak, and D. Vretenar, Phys. Rev. C **95**, 054304 (2017).
[25] I. Dedes and J. Dudek, Acta Phys. Polonica Proceedings Supplement, B **10**, 51 (2017).
[26] I. Dedes and J. Dudek, Phys. Scr. **93**, 044003 (2018).
[27] J. Dudek, B. Szpak, M.-G. Porquet, H. Molique, K. Rybak, and B. Fornal, J. Phys. G: Nucl. Part. Phys. **37**, 064031 (2010).
[28] A similar model used in a different context has been introduced in J. Dudek, B. Szpak, B. Fornal, and A. Dromard, Phys. Scr. **T154**, 014002 (2013).
[29] W. H. Press, S. A. Teukolsky, W. T. Vetterling, and B. P. Flannery, *Numerical Recipes in FORTRAN 77: The Art of Scientific Computing* (Cambridge University, Cambridge, England, 1992).
[30] R. F. Casten, J. Phys. G: Nucl. Part. Phys. **42**, 034029 (2015).
[31] ENSDF data base, https://www.nndc.bnl.gov/ensdf/.
[32] H. Langevin-Joliot, J. van de Wiele, J. Guillot, E. Gerlic, L. H. Rosier, A. Willis, M. Morlet, G. Duhamel-Chretien, E. Tomasi-Gustafsson, N. Blasi, S. Micheletti, and S. Y. van der Werf, Phys. Rev. C **47**, 1571 (1993).

[33] S. Gales, G. M. Crawley, D. Weber, and B. Zwieglinski, Phys. Rev. C **18**, 2475 (1978).
[34] R. F. Casten, E. Cosman, E. R. Flynn, O. Hansen, P. W. Keaton Jr., N. Stein, R. Stock, Nucl. Phys. A **202**, 161 (1973).
[35] S. E. Vigdor, R. D. Rathme, H. S. Liers, and W. Haeberli, Nucl. Phys. A **210**, 70 (1973).
[36] M. Wang, G. Audi, A. H. Wapstra, F. G. Kondev, M. MacCormick, X. Xu, and B. Pfeiffer, Chin. Phys. C **36**, 1603 (2012).